



Article

Elucidating the Effects of Curcumin against Influenza Using In Silico and In Vitro Approaches

Minjee Kim ¹, Hanul Choi ¹, Sumin Kim ² , Lin Woo Kang ² and Young Bong Kim ^{1,*}

¹ Department of Biomedical Science and Engineering, Konkuk University, Seoul 05029, Korea; mj0411@konkuk.ac.kr (M.K.); chlgksmf9977@hanmail.net (H.C.)

² Department of Biological Sciences, Konkuk University, Seoul 05029, Korea; fly0000@naver.com (S.K.); lkang@konkuk.ac.kr (L.W.K.)

* Correspondence: kimera@konkuk.ac.kr; Tel.: +82-2-450-4208

Abstract: The influenza virus is a constantly evolving pathogen that challenges medical and public health systems. Traditionally, curcumin has been used to treat airway inflammatory diseases, such as bronchitis and pneumonia. To elucidate common targets of curcumin and influenza infection and underlying mechanisms, we employed network pharmacology and molecular docking approaches and confirmed results using in vitro experiments. Biological targets of curcumin and influenza were collected, and potential targets were identified by constructing compound–disease target (C–D) and protein–protein interaction (PPI) networks. The ligand–target interaction was determined using the molecular docking method, and in vitro antiviral experiments and target confirmation were conducted to evaluate curcumin’s effects on influenza. Our network and pathway analyses implicated the four targets of AKT1, RELA, MAPK1, and TP53 that could be involved in the inhibitory effects of curcumin on influenza. The binding energy calculations of each ligand–target interaction in the molecular docking showed that curcumin bound to AKT1 with the highest affinity among the four targets. In vitro experiments, in which influenza virus-infected MDCK cells were pre-, co-, or post-treated with curcumin, confirmed curcumin’s prophylactic and therapeutic effects. Influenza virus induction increased the level of mRNA expression of AKT in MDCK cells, and the level was attenuated by curcumin treatment. Collectively, our findings identified potential targets of curcumin against influenza and suggest curcumin as a potential therapy for influenza infection.

Keywords: curcumin; influenza; inflammation; network pharmacology; molecular docking; systems biology



Citation: Kim, M.; Choi, H.; Kim, S.; Kang, L.W.; Kim, Y.B. Elucidating the Effects of Curcumin against Influenza Using In Silico and In Vitro Approaches. *Pharmaceuticals* **2021**, *14*, 880. <https://doi.org/10.3390/ph14090880>

Academic Editor: Daniela De Vita

Received: 28 June 2021

Accepted: 24 August 2021

Published: 30 August 2021

Publisher’s Note: MDPI stays neutral with regard to jurisdictional claims in published maps and institutional affiliations.



Copyright: © 2021 by the authors. Licensee MDPI, Basel, Switzerland. This article is an open access article distributed under the terms and conditions of the Creative Commons Attribution (CC BY) license (<https://creativecommons.org/licenses/by/4.0/>).

1. Introduction

Seasonal influenza A virus (IAV) is an infectious, enveloped, negative-sense, single-strand RNA virus that is the most common cause of pneumonia-related deaths [1]. Initially, a mild respiratory infection targets the upper respiratory tract, characterized by fever, cough, muscle pain, and fatigue, IAV can lead to severe lethal pneumonia owing to secondary bacterial infection of the lower respiratory tract [2]. Frequent updates of influenza vaccines are necessary, owing to mutations in influenza virus glycoproteins that enable evasion of antibody-mediated immunity induced by vaccination [3]. Together with vaccines, antiviral drugs are used for both treating patients and preventing infection in individuals who have been exposed [2]. However, the emergence of drug-resistant viruses is a major challenge in using antiviral drugs; thus, it is still necessary to explore alternative therapeutic approaches for treating influenza infection [4].

Curcumin has attracted considerable research interest because of its versatile pharmacological properties, including anti-inflammatory, antiviral, and anticancer effects [3]. Previous studies have reported that curcumin inhibits the influenza virus by interfering with cellular signaling pathways, including Toll-like receptor and nuclear factor- κ B pathways, and disrupting the viral envelope and liposomal membranes [5,6]. However,

therapeutic targets and underlying mechanisms of curcumin against influenza have not been fully studied.

To identify and predict targets and underlying mechanisms of curcumin against influenza infection, we implemented a computational research approach and further validated *in silico* results *in vitro*. Computational strategies are promising and time-saving alternatives to experimental research that facilitate the identification of targets and disease pathways [7,8]. Herein, we investigated targets associated with curcumin and influenza to determine targets in common, which were further studied through protein–protein interaction (PPI) networks to explore the relationship between the targets. We confirmed biological signaling pathways through the Kyoto Encyclopedia of Genes and Genomes (KEGG) based on common targets. Two networks, compound–disease target (C-D) network and disease target–pathway network (D-P), were constructed and merged to yield a compound–disease target–biological signaling pathway (C-D-P) network to understand underlying mechanisms of curcumin and influenza. A molecular docking study was conducted to evaluate ligand–target interactions between curcumin and proposed targets. Lastly, we performed *in vitro* antiviral assays to determine antiviral effects of curcumin and target confirmation to observe the underlying mechanism of curcumin against influenza infection. Collectively, our *in silico* and *in vitro* approaches identified potent targets and underlying mechanisms of curcumin associated with influenza and established antiviral effects of curcumin.

2. Results

2.1. Biological Targets of Curcumin and Influenza

Overall, 231 *H. sapiens* target genes associated with curcumin were retrieved from DrugBank, GeneCards, and NCBI databases, and 1317 targets associated with influenza virus were identified from DisGeNET and NCBI databases (Figure 1).

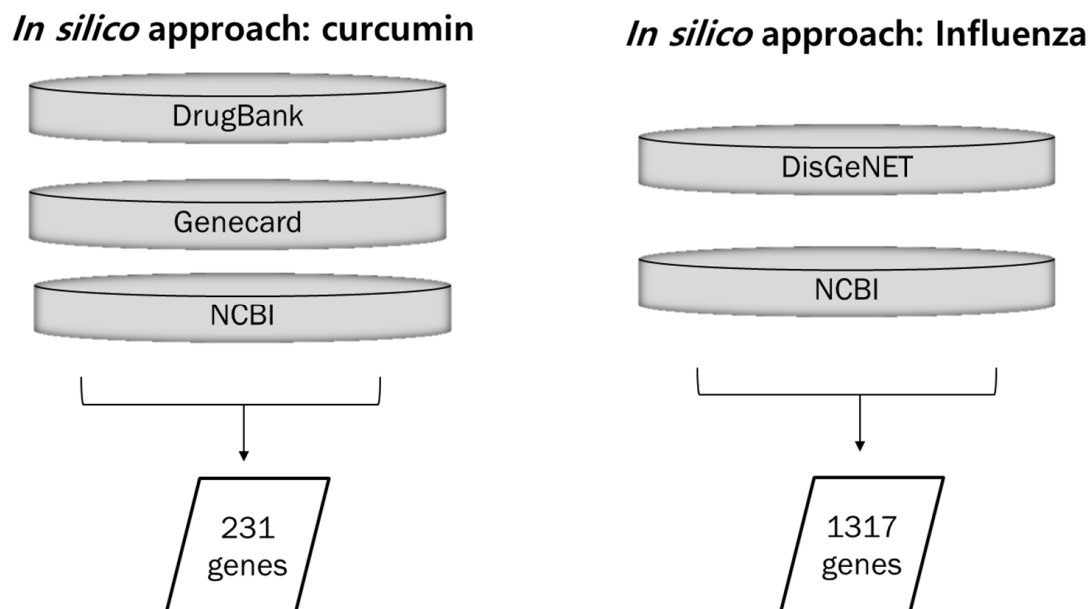


Figure 1. Collection of data for curcumin-, influenza-, and lung inflammation-associated genes. Curcumin-associated genes were collected from three databases: DrugBank, GeneCards, and NCBI. Influenza- and lung inflammation-associated genes were retrieved from two databases: DisGeNET and NCBI.

2.2. Compound–Disease Target Network

Among 231 curcumin and 1317 influenza target genes, 23 targets were retrieved as overlapping genes and constructed as a network using Cytoscape (Figure 2).

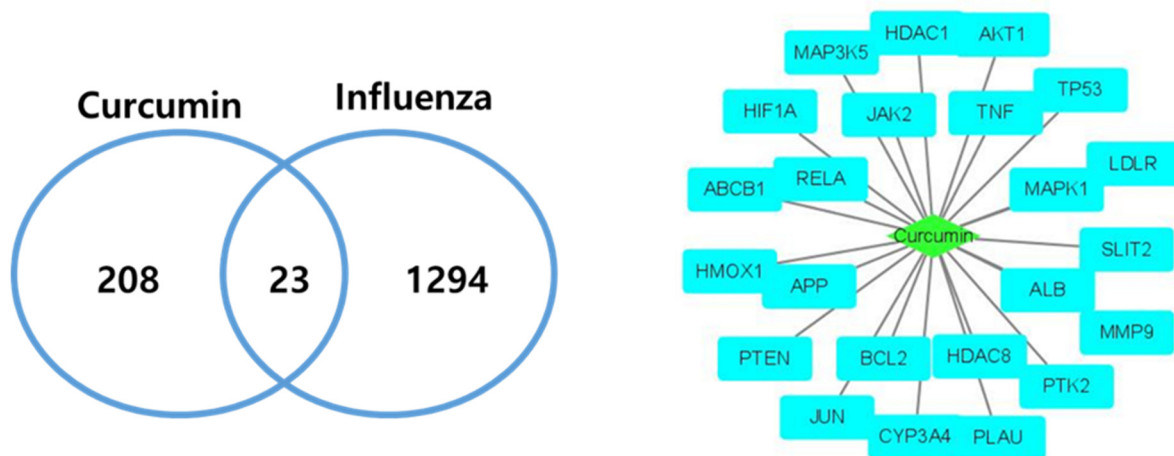


Figure 2. Curcumin–Influenza-associated targets. In total, 23 curcumin and influenza infection common targets were retrieved and constructed as a network.

2.3. KEGG Pathway Analysis

A KEGG enrichment analysis was further performed on the 23 retrieved curcumin–influenza targets using DAVID bioinformatics resources. The top 20 enriched pathways and diseases ($p < 0.05$) based on gene counts were obtained. This analysis revealed that these targets were enriched for seven viral diseases (hepatitis B, toxoplasmosis, Epstein–Barr virus infection, hepatitis C, influenza A, tuberculosis, and viral carcinogenesis), three inflammation-associated pathways (PI3K–AKT, TNF, and MAPK signaling pathways), and cancer (Table 1).

Table 1. Top 20 enriched KEGG pathways and diseases.

Pathway and Disease (KEGG)	Gene Counts
hsa05200: Pathways in cancer	11
hsa05161: Hepatitis B	9
hsa04071: Sphingolipid signaling pathway	8
hsa05205: Proteoglycans in cancer	8
hsa04151: PI3K–AKT signaling pathway	8
hsa04668: TNF signaling pathway	7
hsa05145: Toxoplasmosis	7
hsa04722: Neurotrophin signaling pathway	7
hsa04010: MAPK signaling pathway	7
hsa05206: MicroRNAs in cancer	7
hsa05222: Small cell lung cancer	6
hsa05215: Prostate cancer	6
hsa04066: HIF-1 signaling pathway	6
hsa05169: Epstein–Barr virus infection	6
hsa05160: Hepatitis C	6
hsa05202: Transcriptional misregulation in cancer	6
hsa05164: Influenza A	6
hsa05152: Tuberculosis	6
hsa05203: Viral carcinogenesis	6
hsa04510: Focal adhesion	6

PI3K, phosphoinositide 3-phosphate kinase; TNF, tumor necrosis factor; MAPK, mitogen-activated protein kinase; HIF-1, hypoxia-induced factor 1.

2.4. Protein–Protein Interactions of Disease Targets Associated with Curcumin

A protein–protein interaction (PPI) network was constructed with the STRING database using the 23 target genes as input (Figure 3). The database STRING is a global database for the analysis of functional links between proteins. The genes that encode proteins are

required for the same function are often located in close proximity to the genome. The graphical representation of the network protein interactions provides a functional linkage, facilitating the analysis of modularity in biological processes [9]. The resulting network revealed two main targets: TP53 (tumor protein 53), which was directly connected to 36 nearest neighbors (degree 36), followed by AKT1 (RAC-alpha serine/threonine-protein kinase: degree 29).

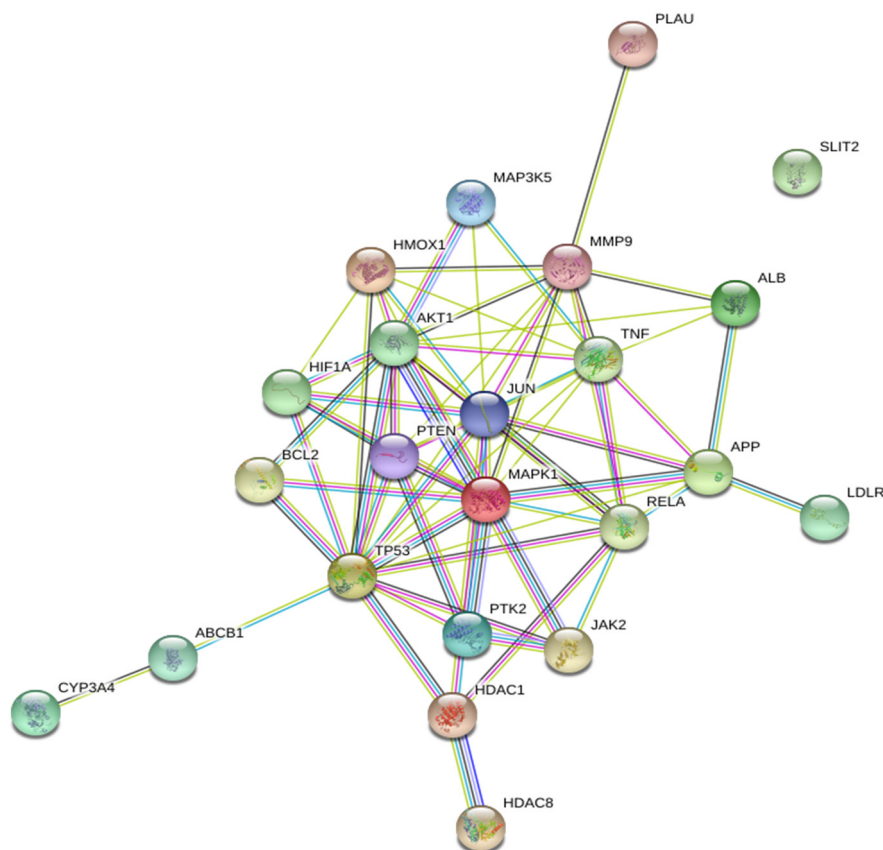


Figure 3. Protein–protein Interaction (PPIs) network constructed using the STRING database. In total, 23 overlapping targets of curcumin and influenza were used as input for the STRING database to construct a PPI network. Two main targets, TP53 (tumor protein 53) and AKT1 (RAC-alpha serine/threonine-protein kinase) were identified in this network.

2.5. Compound–Disease Target–Pathway (C–D–P) Network

Two networks, compound–disease target (C–D) network and disease target–pathway network (D–P) were constructed and merged to yield a C–D–P network (Figure 4). The C–D–P network contains 45 nodes and 162 edges. The green diamond in the center, sky blue rectangles, and light purple oblongs correspond to compound, disease targets, and pathways, respectively. Our network analysis showed that AKT1 and RELA (transcription factor p65) exhibited the highest connectedness (degree 18), followed by mitogen-activated protein kinase 1 (MAPK1) (degree 17) and TP53 (degree 15).

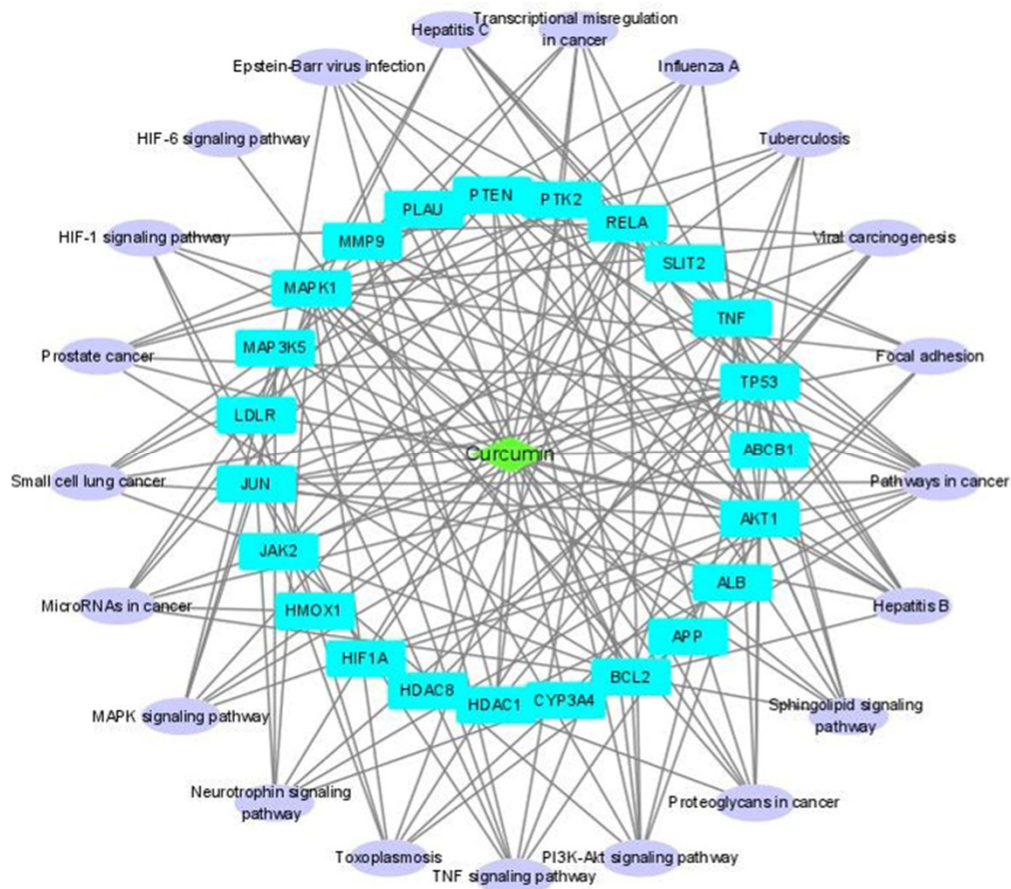


Figure 4. Compound–disease target–pathway (C-D-P) network. C-D network and D-P network were constructed and merged to produce the C-D-P network using Cytoscape.

2.6. Molecular Docking Analysis

From our two network results (Figures 3 and 4), we selected four proteins—AKT1, TP53, MAPK1, and RELA—as potential targets for curcumin against influenza-associated inflammation. A ligand–target docking approach was used to study the binding affinity (kcal/mol) between curcumin and the targets. The following structures of curcumin and targets were used in the molecular docking: curcumin (the keto form, PDB ID: 6HDR and the enol form, 4PMF); AKT-1 (3O96) [10]; TP53 (3LH0) [11]; MAPK1 (2OJJ) [12]; RELA (1NFI) [13]. The overall structures of the selected target are well conserved with those of the same proteins in different PDBs (Supplementary Table S1). Curcumin exists in two tautomeric forms (keto and enol) [14]; thus, we investigated both forms with the identified targets. The calculated binding affinity (kcal/mol) of each ligand–target identified that curcumin and AKT1 show the strongest binding affinity among all the ligand–target pairs (Table 2).

Table 2. The calculated binding affinity of ligand–target.

Ligand–Target	Binding Affinity (kcal/mol) (KETO)	Binding Affinity (kcal/mol) (ENOL)
CM-AKT1	−9.2	−9.0
CM-TP53	−7.0	−7.1
CM-MAPK1	−7.0	−6.9
CM-RELA	−6.9	−7.0

CM, curcumin, KETO: keto form of curcumin, ENOL: enol form of curcumin.

For the molecular docking, we selected structures in complex with a small molecule (ligand) as the representative structure of each target. The bound ligand was extracted from the original structure and redocked to the same macromolecule. The RMSD value between the structures of original and redocked ligands was measured and used for the validation of the docking protocol. The docking using AutoDock Vina successfully identified the original binding conformations of the ligands in all targets except RELA (Supplementary Table S2). There is no small-molecule ligand-bound structure of RELA. All the RMSD values (Å) of the redocked original ligand from the crystallographic structures were 0.000, which were listed as top solutions in the Supplementary Table S2. In our study, the lowest predicted binding affinity that had RMSD values of zero was selected.

Ligand–receptor interactions were identified using Discovery Studio visualizer and verified in Pymol (Figure 5). Curcumin–AKT1 interactions were further analyzed with both the keto (cyan) and enol (yellow) forms of curcumin. Curcumin is a symmetric molecule. In the docked model, half of the curcumin is tightly bound in AKT1, and the other half is partially exposed to solvent (Figure 5A). The internally bound half of curcumin has extensive hydrophobic interactions with Ile36, Phe55, and Tyr326. The other solvent-exposed half of curcumin has the van der Waals interactions with Leu52, Gly327, Arg328, and Pro388. Both keto and enol forms of curcumin show the conserved binding conformation except the rotation of the main chain having the different keto and enol motifs. The curcumin (keto)–AKT1 interaction involves three hydrogen bonds with the key residues Gly37, Asp323, and Arg328, and the van der Waals interactions with Lys14, Arg25, Arg86, Arg328, and Ala329 (Figure 5B). The curcumin (enol)–AKT1 interaction formed two hydrogen bonds with the key residues Gly37 and Tyr326, and the van der Waals interactions with Lys14, Arg86, Ile36, and Ile84 (Figure 5C).

In AKT1, the docking result of the two forms of curcumin was compared to that of the original ligand, AKT1 inhibitor (IQO), in the selected AKT1 structure (PDB ID: 3O96) (Table 3) [10]. The AKT1 inhibitor shows a very low binding energy of <-14.0 Kcal/mol and curcumin also shows reasonable binding energy of <-9.0 Kcal/mol, compared to the previously published docking study [15].

Table 3. Ligand–target binding affinity, compared to AKT inhibitor IQO.

Ligand–Target	Binding Affinity (kcal/mol)
CM(keto)-AKT1	−9.2
CM(enol)-AKT1	−9.0
IQO (AKT inhibitor)-AKT1	−14.4

2.7. Concentration-Dependent Cytotoxic Effects of Curcumin and Oseltamivir against Influenza Virus

MDCK cells were treated with curcumin and oseltamivir (positive control) for 48 h and stained with crystal violet, after which optical density (OD) was measured at 575 nm using a spectrophotometer. The calculated CC_{50} values of curcumin and oseltamivir were 61.27 and 310.2 μ M, respectively (Table 4).

Table 4. Cytotoxic effects of curcumin in MDCK cells.

Compound	CC_{50} (μ M)
Curcumin	61.27 \pm 1.69
Oseltamivir	310.2 \pm 1.55

CC_{50} , 50% cytotoxic concentration ($n = 3$).

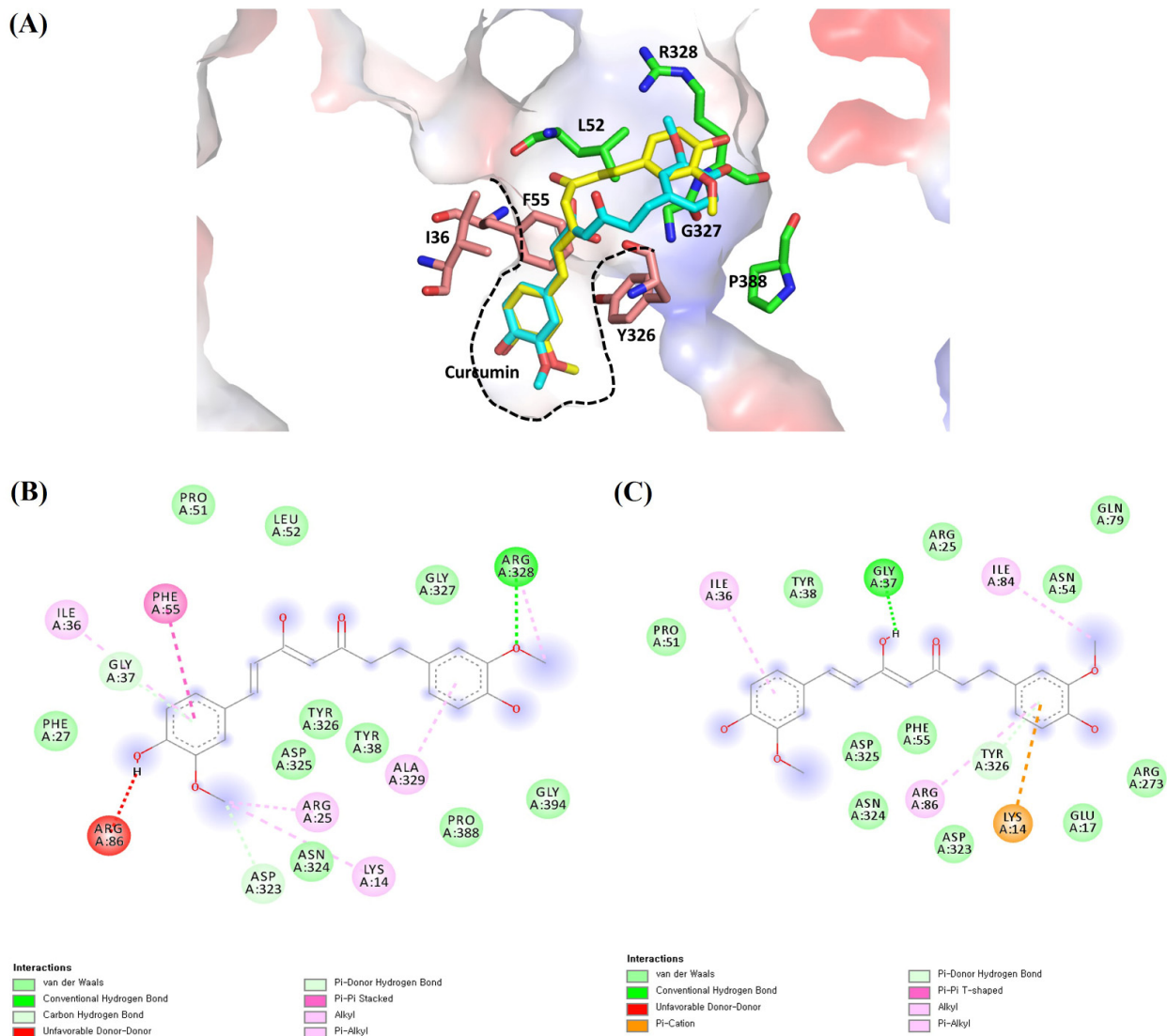


Figure 5. The proposed ligand–receptor interactions of curcumin–AKT1 from molecular docking: (A) ligand–receptor interactions of the keto (cyan) and enol (yellow) forms of curcumin with AKT1 showing the electrostatic surface in the 3D representation. Half of the curcumin is tightly bound in AKT1 with the hydrophobic residues (pink) of Ile36, Phe55, and Y326, and the other half is partially exposed to solvent and interacts with the surface residues (green) of Leu52, Gly327, Arg328, and Pro388. The tight hydrophobic pocket is shown in the dashed black line; (B) the detailed molecular interactions of the keto form of curcumin with AKT1 in the 2D representation; (C) the detailed molecular interactions of the enol form of curcumin with AKT1 in the 2D representation.

To measure the anti-influenza actions of curcumin in MDCK cells, we assessed its effect on the virus cycle by performing antiviral experiments using three paradigms: pre-treatment, co-treatment, and post-treatment. In antiviral tests, MDCK cells infected with the influenza virus (100TCID₅₀) were treated with different concentrations of curcumin (3.125–30 μM) according to the indicated paradigm (Figure 6). The greatest effect was observed with pre-treatment, which increased cell viability to more than 50% at concentrations as low as 3.75 μM. Post-treatment also significantly enhanced cell survival at concentrations of 30 and 15 μM, but co-treatment had no effect at any concentration. Collectively, these experiments confirm that curcumin exerts antiviral effects against the influenza virus when applied as a pre-treatment or post-treatment, suggesting that curcumin may be effective in both prophylactic and therapeutic applications.

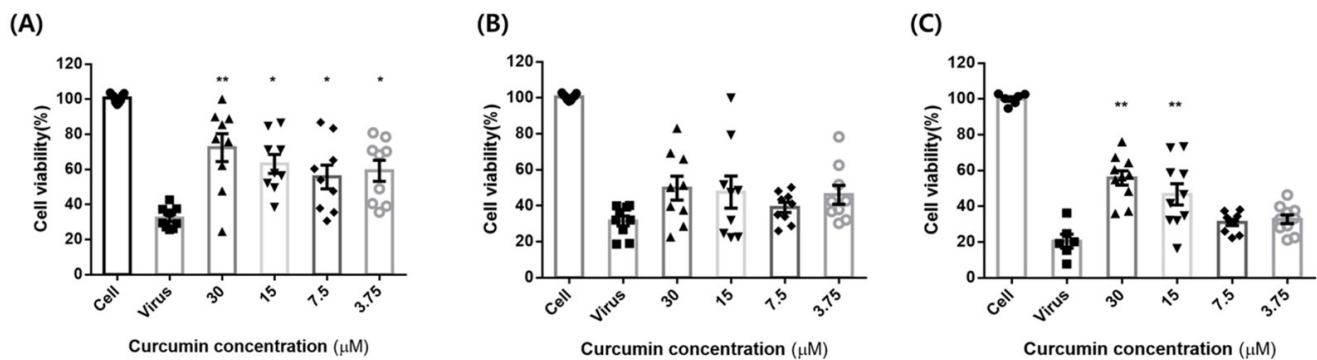


Figure 6. Curcumin cytopathic effect (CPE) test. MDCK cells were treated with influenza virus (100TCID₅₀) with or without different concentrations of curcumin (3.125–30 μ M): (A) pre-treatment: MDCK cells were pre-treated with different concentrations of curcumin for 1 h at 37 $^{\circ}$ C and then infected with influenza virus for 48 h to determine curcumin's prophylactic effect; (B) co-treatment: MDCK cells infected with virus were co-treated with different concentrations of curcumin for 48 h at 37 $^{\circ}$ C to determine curcumin's virus binding-inhibitory effect; (C) post-treatment: MDCK cells were infected with virus for 1 h and then incubated with curcumin for 48 h at 37 $^{\circ}$ C to validate whether curcumin exhibits therapeutic effects. ** $p < 0.001$, * $p < 0.05$, compared with the virus group; NS, not significant.

2.8. Inhibitory Effects of Curcumin on Influenza Virus-Induced AKT mRNA Expression

The impact of influenza infection on activation of AKT mRNA expression was confirmed by qRT-PCR (Figure 7). The levels of AKT were significantly attenuated by curcumin in all three treatment methods (pre-, co-, and post-treatment). The greatest effect was observed with pre-treatment, which corresponds to our antiviral study.

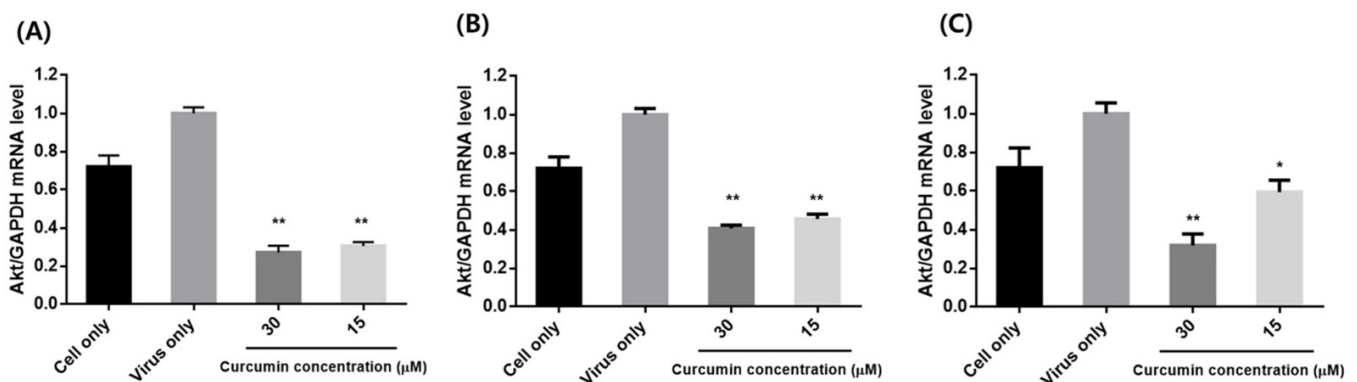


Figure 7. Effects of curcumin treatment on mRNA expression of AKT in influenza-infected MDCK cells: (A) pre-treatment: MDCK cells were pre-treated with different concentrations (15 and 30 μ M) of curcumin and infected with influenza virus; (B) co-treatment: MDCK cells infected with virus were co-treated with different concentrations of curcumin; (C) post-treatment: MDCK cells were infected with virus and then incubated with curcumin. ** $p < 0.001$, * $p < 0.05$, compared with the virus group.

3. Discussion

In the present study, we conducted a systems biology investigation (in silico), antiviral assay study, and target confirmation (in vitro) of curcumin against the influenza virus. We identified four targets—AKT1, RELA, MAPK1 and TP53—from our C-D-P network analysis, and two targets—TP53 and AKT1—from our PPI network that showed high degrees of interactions in silico. All targets are involved in a wide variety of cellular processes and metabolism. AKT proteins regulate cellular functions including cell proliferation, survival, metabolism, and angiogenesis [16]. RELA encodes the NF- κ B subunit, a transcription factor that is initiated by many biological processes such as inflammation, immunity, differentiation, cell growth, tumorigenesis, and apoptosis [17]. MAP kinases are also involved in

proliferation, differentiation, transcription regulation, and development [18]. PI3K/AKT and downstream of Toll-like receptors (TLRs), MAPK/NF- κ B signaling pathways have been proved to be involved in IAV replication [19,20]. A previous study reported that curcumin significantly suppressed IAV-induced activation of TLR2/4/7, AKT, p38/JNK MAPK, and NF- κ B pathways [5]. Another study group reported that curcumin inhibited NF- κ B signaling in macrophages, and the production of cytokines/chemokines responding to IAV infection, which corresponds to our result [4]. TP53-encoded proteins respond to diverse cellular stresses to regulate the expression of target genes, thereby inducing cell cycle arrest, apoptosis, senescence, DNA repair, or changes in metabolism [21]. In response to IAV infection, p53 is accumulated and activated, responsible for regulating apoptosis and host antiviral defense [22]. In resting cells, low levels of p53 are maintained due to its interactions with the E3 ubiquitin ligase, MDM2 by continuous proteasomal degradation [22]. IAV infection is reported to weaken the interaction between MDM2 and p53, leading increased level of p53 [22]. Curcumin has been identified as an inhibitor of MDM2 that acts independently of p53 [23]. The inhibitory effects of MDM2 occur at the transcriptional level and appear to involve the PI3K/mammalian target of rapamycin (mTOR)/erythroblastosis virus transcription factor 2 (ETS2) pathway [23]. In this regard, upon curcumin-induced inhibition of MDM2 expression, influenza virus infection may lose its target of interaction, resulting in reduced infection.

Our pathway study identified seven virus-associated diseases, including influenza (tuberculosis, viral carcinogenesis, hepatitis B and C, toxoplasmosis, Epstein–Barr virus infection, and influenza) and three inflammation-associated pathways (PI3K-AKT, TNF, and MAPK signaling pathways). Moreover, our molecular docking study showed that, among the four identified targets, AKT1 showed the highest binding affinity for curcumin, indicating that AKT1 is the most potent target. The calculated binding energy of curcumin to AKT1 was reasonably low as <-9.0 Kcal/mol, indicating a possible inhibitory effect [15]. Lastly, our in vitro study demonstrated that curcumin was effective against influenza virus in both pre- and post-treatment paradigms, and confirmed inhibition of mRNA level of AKT expression suggesting that curcumin could be useful as either a prophylactic or therapeutic influenza agent.

Curcumin, isolated from the rhizome of *Curcuma longa* L. (turmeric), is widely recognized for its anti-inflammatory, antimicrobial, and anticancer effects [24]. Due to its versatile pharmacological properties, curcumin has been considered as another option to replace current influenza therapy [6]. Previous studies reported that curcumin inhibits influenza infection by interfering with multiple cellular signaling pathways, but therapeutic targets and underlying mechanisms of action of curcumin against influenza have not been fully elucidated. Herein, our network study identified three main pathways associated with curcumin and influenza: PI3K/AKT, TNF, and MAPK signaling pathways. Among these pathways, the PI3K/AKT pathway stands out in the context of our identification of AKT1 as a target. PI3K consists of a regulatory subunit (p85) and a catalytic subunit (p110) and is activated by autophosphorylation following binding of the Src homology (SH) domain in p85 to viral proteins in the cytoplasm [25]. Upon activation, PI3K phosphorylates lipid substrates of p110, which serve as second messengers to regulate AKT [26]. AKT plays a central role in modulating cellular pathways such as cell survival, proliferation, and apoptosis [27]. It is also involved in influenza virus uptake and later stages of the virus replication cycle [28]. It has been shown that apoptosis in influenza-infected MDCK cells is AKT dependent and is downregulated by the viral protein NS1, an inducer of host AKT [29]. According to Ehrhardt et al., PI3K targets a very early step of the viral replication cycle [30]. Immunofluorescence microscopy analyses indicated that PI3K is involved in the regulation of virus uptake, as indicated by the accumulation of virus particles at the cell surface upon inhibition of PI3K [30]. Another study group reported that inhibition of the PI3K/AKT pathway in influenza infection leads to a reduction in virus yield, further demonstrating a decrease in viral RNA and protein synthesis that suggested a role for the PI3K/AKT pathway in a late phase of infection, such as virus replication [31]. Overall, these reports

support our pathway (PI3K/AKT) and target (AKT1) results for curcumin and influenza, as well as our *in vitro* study of prophylactic and therapeutic effects of curcumin and AKT target confirmation. It was also reported that curcumin downregulates PI3K/AKT signaling during the lipopolysaccharide (LPS)-induced inflammatory response in microglial cells, indicating that curcumin may inhibit influenza virus infection by regulating the PI3K/AKT pathway and that AKT1 could be a potential target in preventing influenza virus [32].

4. Materials and Methods

4.1. Systems Biology

4.1.1. Pharmacokinetic Evaluation and Therapeutic Targets Associated with Curcumin

Therapeutic targets of curcumin were obtained from DrugBank (ver.5.1.4, University of Alberta, Alberta, Canada) [33], GeneCards (ver.5.1.4, Weizmann Institute of Science, Rehovot, Israel) [34], and NCBI databases (National Center for Biotechnology Information, U.S. National Library of Medicine, Bethesda, MD, USA) [35]. All searches were performed with “Homo sapiens” selected.

4.1.2. Potential Pathological Target Genes Linked to Influenza and Inflammation

Influenza infection- and lung inflammation-associated targets were obtained from DisGeNET (ver.7.0, Research Programme on Biomedical Informatics (GRIB), Spain) [36] and NCBI databases [35]. All searches were performed with “Homo sapiens” selected.

4.1.3. Construction of a Compound–Disease Target (C-D) Network

Overlapping genes between curcumin (compound) and disease targets (influenza and lung inflammation) were retrieved and constructed as a network using Cytoscape (ver.3.8, Institute for systems biology, Seattle, WA, USA) [37].

4.1.4. Biological Function and Pathway Enrichment Analysis

Pathways associated with identified target proteins were retrieved from the Database for Annotation, Visualization and Integrated Discovery (DAVID ver. 6.8, National Cancer Institute at Frederick, Frederick, MD, USA) database [38]. Analyses using this database apply statistical approaches to identify significantly enriched or depleted groups of selected genes or proteins. A pathway enrichment analysis was performed using the Kyoto Encyclopedia of Genes and Genomes (KEGG) database (release 99.0, Kyoto University, Kyoto, Japan) [39].

4.1.5. Construction of Protein–Protein Interaction (PPI) Network

Search Tool for Retrieval of Interacting Genes/Proteins database (STRING ver.11.0, Swiss Institute of Bioinformatics, Basel, Switzerland) [40] was used to collect target and target interactions with confidence scores > 0.7, and the network was analyzed using Cytoscape [37].

4.1.6. Compound–Disease Target–Pathway (C-D-P) Network Construction

Curcumin–disease target and disease target–pathway networks were constructed and visualized using Cytoscape [37]. Pathways with *p*-values < 0.05 were used in this network. The two constructed networks were analyzed and merged to produce a compound–disease target–pathway (C-D-P) network.

4.1.7. Molecular Docking Analysis

A ligand–target docking approach was used to analyze structural complexes of targets with ligands to understand target specificity. Three-dimensional (3D) structures of targets were downloaded from the RCSB protein data bank (University of California San Diego, La Jolla, CA, USA) [41]. Curcumin exists in two tautomeric forms (keto and enol) [14]. The chemical structures of both forms of curcumin were extracted from X-ray crystal form from the RCSB protein data bank (the keto form, PDB ID: 6HDR [42], and the enol form, PDB

ID: 4PMF [43]) using Pymol (ver.2.4.0) [44]. All the structures of targets and ligands were converted to the suitable form of PDB using the Avogadro program (ver.1.90.0, University of Pittsburgh, Pittsburgh, PA, USA) [45] and Discovery Studio [46]. For molecular docking, heteroatoms and waters were deleted, and polar hydrogens were added to the original structure of targets. Docking was carried out with AutoDock Vina (ver.1.1.2, Center of Computational Structural Biology (CCSB)—Scripps Research, CA, USA) [47] using PyRx (ver.0.9.6, Scripps Research, La Jolla, CA, USA) [48] based on scoring functions. The Computer Atlas of Surface Topology of proteins (CASTp) server (ver 3.0, University of Illinois at Chicago, Chicago, IL, USA) [49] was used to locate active site of targets. The 2D- and 3D ligand–target interactions were retrieved using BIOVIA Discovery Studio (ver.4.5, BIOVIA, CA, USA) [46]. To validate the molecular docking, the ligands bound to targets in the selected PDBs were extracted, redocked in the same target structures, and the correlation between the original and redocked structures of ligands was confirmed with the root mean square deviation (RMSD) value.

4.2. *In Vitro* Experiments

4.2.1. Plant Material and Reagents

Curcumin was purchased from CSN Pharm (Arlington Heights, IL, USA), and purity (>99%) was confirmed by the manufacturer. Curcumin was dissolved in dimethyl sulfoxide (DMSO) to generate a 10 mM stock solution. Dulbecco's modified Eagle medium (DMEM) was purchased from HyClone (Logan, UT, USA), and fetal bovine serum (FBS) was obtained from Gibco (Carlsbad, CA, USA).

4.2.2. Cells and Viruses

The influenza virus, H1N1 (A/Puerto Rico/8/34), was provided by professor Song Chang Sun (College of Veterinary Medicine, Konkuk University, Korea), and Madin-Darby canine kidney (MDCK) cells were purchased from the Korean Cell Line Bank (KCLB, Seoul, Korea). MDCK cells were cultured in DMEM containing 10% FBS and 1% penicillin–streptomycin at 37 °C in a humidified 5% CO₂ atmosphere. Influenza viruses were cultured in DMEM containing 0.3% BSA, 1 µg/mL trypsin and 1% penicillin–streptomycin at 37 °C and 5% CO₂. Virus titers were determined using the 50% tissue culture infectious dose (TCID₅₀) according to the Reed and Muench endpoint method.

4.2.3. Detection of Cytotoxicity

MDCK cells were seeded into 96-well plates at a concentration of 1×10^4 cells/well. After 24 h, cells were treated with serial dilutions of curcumin for 48 h 37 °C and then stained with crystal violet. Cell viability at each concentration was determined by measuring the optical density (OD) at 575 nm using a spectrophotometer, and the CC₅₀ value, defined as the concentration that induced 50% cell death, was determined. Oseltamivir was used as a positive control.

4.2.4. Antiviral Assay: Pre-Treatment, Co-Treatment, and Post-Treatment

MDCK cells were seeded in a 96-well plate (1×10^4 cells/well) and, after 24 h, were treated with the indicated concentrations of curcumin and infected with 100TCID₅₀ of influenza virus. Antiviral effects of curcumin were evaluated using three methods: (a) pre-treatment, carried out by preincubation of cells with curcumin for 1 h at 37 °C and then incubation with influenza; (b) co-treatment, performed by incubating influenza and curcumin together for 1 h at 37 °C; (c) post-treatment, conducted by preincubation of cells with influenza for 1 h at 37 °C, followed by incubation with curcumin for 1 h at 37 °C. After incubating for 2 d, cells were stained with crystal violet, and optical density (OD) at 575 nm was measured using a spectrophotometer.

4.2.5. Quantitative Real-Time PCR: Pre-Treatment, Co-Treatment, and Post-Treatment

MDCK cells were seeded in a 6-well plate (5×10^5 cells/well) with curcumin (15 and 30 μM) by pre-, co-, and post-treatment and infected with influenza virus. Total RNA was isolated by RNeasy Mini kit (Qiagen, CA, USA) from MDCK cells, and 1 μg of the total RNA was reverse-transcribed into cDNA with the SuperScript II reverse transcriptase (Invitrogen, Carlsbad, CA, USA). Quantitative real-time PCR (qRT-PCR) was performed with a SsoAdvanced Universal SYBR[®] Green Supermix kit (Bio-Rad, Hercules, CA, USA). Cycling parameters of the qPCR were as follows: 1 cycle at 95 °C for 3 min, followed by 39 cycles at 95 °C for 10 s, 60 °C for 30 s in the on the LightCycler 96 system (Roche, Mannheim, Germany). Primer sequences were as follows: AKT forward, 5'-CAA GTC CTT GCT TTC AGGGC-3' and reverse, 5'-ATA CCT GGT GTC AGT CTC CGA-3' (184-bp product); GAPDH forward, 5'-TGT CCC CAC CCC CAA TGT ATC-3' and reverse, 5'-CTC CGA TGC CTG CTT CAC TAC CTT-3' (100-bp product). Expression levels of the AKT gene were normalized to glyceraldehyde-3-phosphate dehydrogenase (GAPDH).

4.2.6. Statistical Analysis

All data were analyzed using the GraphPad Prism6 software (GraphPad Software Inc., San Diego, CA, USA), and a value of $p < 0.05$ was considered statistically significant. The measurements were assessed by one- or two-way ANOVA.

5. Conclusions

In summary, through an in silico study, we identified AKT1 as a potential target and the PI3K/AKT pathway as possibly the main pathway associated with curcumin's action against influenza. We also demonstrated the prophylactic and therapeutic effects of curcumin in vitro and confirmed AKT inhibition by curcumin treatment indicating curcumin's potential in treating influenza via AKT inhibition. Given the wide availability of curcumin, there should be no significant barriers to clinical trials, which are warranted to confirm curcumin as a future influenza treatment.

Supplementary Materials: The following are available online at <https://www.mdpi.com/article/10.3390/ph14090880/s1>, Table S1: The structural similarity between the selected target structures used in docking and other structures of the same targets in PDB. Table S2: RMSD values between the structures of the original and redocked ligands.

Author Contributions: Conceptualization, visualization, methodology, data curation, and writing—original draft preparation, M.K.; in vitro investigation, data curation, and validation, H.C.; visualization, S.K.; data curation, and validation, L.W.K.; writing—review and editing, supervision, and funding acquisition, Y.B.K. All authors have read and agreed to the published version of the manuscript.

Funding: This research was funded by Konkuk University in 2018.

Institutional Review Board Statement: Not applicable.

Informed Consent Statement: Not applicable.

Data Availability Statement: Data sharing contains in this article and supplementary materials.

Conflicts of Interest: The authors declare no conflict of interest.

References

1. Herold, S.; Becker, C.; Ridge, K.M.; Budinger, G.R. Influenza virus-induced lung injury: Pathogenesis and implications for treatment. *Eur. Respir. J.* **2015**, *45*, 1463–1478. [[CrossRef](#)]
2. Krammer, F.; Smith, G.J.D.; Fouchier, R.A.M.; Peiris, M.; Kedzierska, K.; Doherty, P.C.; Palese, P.; Shaw, M.L.; Treanor, J.; Webster, R.G.; et al. Influenza. *Nat. Rev. Dis. Primers* **2018**, *4*, 3. [[CrossRef](#)]
3. Krammer, F. The human antibody response to influenza A virus infection and vaccination. *Nat. Rev. Immunol.* **2019**, *19*, 383–397. [[CrossRef](#)] [[PubMed](#)]
4. Han, S.; Xu, J.; Guo, X.; Huang, M. Curcumin ameliorates severe influenza pneumonia via attenuating lung injury and regulating macrophage cytokines production. *Clin. Exp. Pharmacol. Physiol.* **2018**, *45*, 84–93. [[CrossRef](#)] [[PubMed](#)]

5. Dai, J.; Gu, L.; Su, Y.; Wang, Q.; Zhao, Y.; Chen, X.; Deng, H.; Li, W.; Wang, G.; Li, K. Inhibition of curcumin on influenza A virus infection and influenzal pneumonia via oxidative stress, TLR2/4, p38/JNK MAPK and NF- κ B pathways. *Int. Immunopharmacol.* **2018**, *54*, 177–187. [[CrossRef](#)]
6. Lai, Y.; Yan, Y.; Liao, S.; Li, Y.; Ye, Y.; Liu, N.; Zhao, F.; Xu, P. 3D-quantitative structure-activity relationship and antiviral effects of curcumin derivatives as potent inhibitors of influenza H1N1 neuraminidase. *Arch. Pharmacol. Res.* **2020**, *43*, 489–502. [[CrossRef](#)]
7. Yu, H.; Chen, J.; Xu, X.; Li, Y.; Zhao, H.; Fang, Y.; Li, X.; Zhou, W.; Wang, W.; Wang, Y. A systematic prediction of multiple drug-target interactions from chemical, genomic, and pharmacological data. *PLoS ONE* **2012**, *7*, e37608. [[CrossRef](#)]
8. Shawky, E. Prediction of potential cancer-related molecular targets of North African plants constituents using network pharmacology-based analysis. *J. Ethnopharmacol.* **2019**, *238*, 111826. [[CrossRef](#)]
9. Mering, C.V.; Huynen, M.; Jaeggi, D.; Schmidt, S.; Bork, P.; Snel, B. STRING: A database of predicted functional associations between proteins. *Nucleic Acids Res.* **2003**, *31*, 258–261. [[CrossRef](#)]
10. Wu, W.-I.; Voegtli, W.C.; Sturgis, H.L.; Dizon, F.P.; Vigers, G.P.A.; Brandhuber, B.J. Crystal Structure of Human AKT1 with an Allosteric Inhibitor Reveals a New Mode of Kinase Inhibition. *PLoS ONE* **2010**, *5*, e12913. [[CrossRef](#)] [[PubMed](#)]
11. Joint Center for Structural Genomics (JCSG). Crystal structure of putative hydrolase (YP_751971.1) from *Shewanella frigidimarina* NCIMB 400 at 1.0 Å resolution. In *Joint Center for Structural Genomics (JCSG)*; The Scripps Research Institute: La Jolla, CA, USA, 2010.
12. Aronov, A.M.; Baker, C.; Bemis, G.W.; Cao, J.; Chen, G.; Ford, P.J.; Germann, U.A.; Green, J.; Hale, M.R.; Jacobs, M.; et al. Flipped out: Structure-guided design of selective pyrazolylpyrrole ERK inhibitors. *J. Med. Chem.* **2007**, *50*, 1280–1287. [[CrossRef](#)] [[PubMed](#)]
13. Jacobs, M.D.; Harrison, S.C. Structure of an IkappaBalpha/NF-kappaB complex. *Cell* **1998**, *95*, 749–758. [[CrossRef](#)]
14. Liu, M.; Yuan, M.; Luo, M.; Bu, X.; Luo, H.B.; Hu, X. Binding of curcumin with glyoxalase I: Molecular docking, molecular dynamics simulations, and kinetics analysis. *Biophys. Chem.* **2010**, *147*, 28–34. [[CrossRef](#)]
15. Dotolo, S.; Cervellera, C.; Russo, M.; Russo, G.L.; Facchiano, A. Virtual Screening of Natural Compounds as Potential PI3K-AKT1 Signaling Pathway Inhibitors and Experimental Validation. *Molecules* **2021**, *26*, 492. [[CrossRef](#)]
16. Testa, J.R.; Tschlis, P.N. AKT signaling in normal and malignant cells. *Oncogene* **2005**, *24*, 7391–7393. [[CrossRef](#)]
17. Liu, T.; Zhang, L.; Joo, D.; Sun, S.C. NF- κ B signaling in inflammation. *Signal Transduct. Target. Ther.* **2017**, *2*, 14. [[CrossRef](#)]
18. Zhang, W.; Liu, H.T. MAPK signal pathways in the regulation of cell proliferation in mammalian cells. *Cell Res.* **2002**, *12*, 9–18. [[CrossRef](#)]
19. Hirata, N.; Suizu, F.; Matsuda-Lennikov, M.; Edamura, T.; Bala, J.; Noguchi, M. Inhibition of AKT kinase activity suppresses entry and replication of influenza virus. *Biochem. Biophys. Res. Commun.* **2014**, *450*, 891–898. [[CrossRef](#)] [[PubMed](#)]
20. Marchant, D.; Singhera, G.K.; Utokaparch, S.; Hackett, T.L.; Boyd, J.H.; Luo, Z.; Si, X.; Dorscheid, D.R.; McManus, B.M.; Hegele, R.G. Toll-like receptor 4-mediated activation of p38 mitogen-activated protein kinase is a determinant of respiratory virus entry and tropism. *J. Virol.* **2010**, *84*, 11359–11373. [[CrossRef](#)]
21. Mijit, M.; Caracciolo, V.; Melillo, A.; Amicarelli, F.; Giordano, A. Role of p53 in the Regulation of Cellular Senescence. *Biomolecules* **2020**, *10*, 420. [[CrossRef](#)]
22. Wang, B.; Lam, T.H.; Soh, M.K.; Ye, Z.; Chen, J.; Ren, E.C. Influenza A Virus Facilitates Its Infectivity by Activating p53 to Inhibit the Expression of Interferon-Induced Transmembrane Proteins. *Front. Immunol.* **2018**, *9*, 1–16. [[CrossRef](#)] [[PubMed](#)]
23. Li, M.; Zhang, Z.; Hill, D.L.; Wang, H.; Zhang, R. Curcumin, a dietary component, has anticancer, chemosensitization, and radiosensitization effects by down-regulating the MDM2 oncogene through the PI3K/mTOR/ETS2 pathway. *Cancer Res.* **2007**, *67*, 1988–1996. [[CrossRef](#)]
24. Aggarwal, B.B.; Sethi, G.; Ahn, K.S.; Sandur, S.K.; Pandey, M.K.; Kunnumakkara, A.B.; Sung, B.; Ichikawa, H. Targeting signal-transducer-and-activator-of-transcription-3 for prevention and therapy of cancer: Modern target but ancient solution. *Ann. N. Y. Acad. Sci.* **2006**, *1091*, 151–169. [[CrossRef](#)] [[PubMed](#)]
25. Street, A.; Macdonald, A.; Crowder, K.; Harris, M. The Hepatitis C virus NS5A protein activates a phosphoinositide 3-kinase-dependent survival signaling cascade. *J. Biol. Chem.* **2004**, *279*, 12232–12241. [[CrossRef](#)]
26. Toker, A.; Cantley, L.C. Signalling through the lipid products of phosphoinositide-3-OH kinase. *Nature* **1997**, *387*, 673–676. [[CrossRef](#)] [[PubMed](#)]
27. Datta, S.R.; Brunet, A.; Greenberg, M.E. Cellular survival: A play in three AKTs. *Genes Dev.* **1999**, *13*, 2905–2927. [[CrossRef](#)]
28. Denisova, O.V.; Söderholm, S.; Virtanen, S.; Von Schantz, C.; Bychkov, D.; Vashchinkina, E.; Desloovere, J.; Tynell, J.; Ikonen, N.; Theisen, L.L.; et al. AKT inhibitor MK2206 prevents influenza pH1N1 virus infection in vitro. *Antimicrob. Agents Chemother.* **2014**, *58*, 3689–3696. [[CrossRef](#)]
29. Zhirnov, O.P.; Klenk, H.D. Control of apoptosis in influenza virus-infected cells by up-regulation of AKT and p53 signaling. *Apoptosis* **2007**, *12*, 1419–1432. [[CrossRef](#)]
30. Ehrhardt, C.; Marjuki, H.; Wolff, T.; Nurnberg, B.; Planz, O.; Pleschka, S.; Ludwig, S. Bivalent role of the phosphatidylinositol-3-kinase (PI3K) during influenza virus infection and host cell defence. *Cell. Microbiol.* **2006**, *8*, 1336–1348. [[CrossRef](#)]
31. Shin, Y.K.; Liu, Q.; Tikoo, S.K.; Babiuk, L.A.; Zhou, Y. Effect of the phosphatidylinositol 3-kinase/AKT pathway on influenza A virus propagation. *J. Gen. Virol.* **2007**, *88 Pt 3*, 942–950. [[CrossRef](#)]
32. Cianciulli, A.; Calvello, R.; Porro, C.; Trotta, T.; Salvatore, R.; Panaro, M.A. PI3k/AKT signalling pathway plays a crucial role in the anti-inflammatory effects of curcumin in LPS-activated microglia. *Int. Immunopharmacol.* **2016**, *36*, 282–290. [[CrossRef](#)]

33. Wishart, D.S.; Knox, C.; Guo, A.C.; Shrivastava, S.; Hassanali, M.; Stothard, P.; Chang, Z.; Woolsey, J. DrugBank: A comprehensive resource for in silico drug discovery and exploration. *Nucleic Acids Res.* **2006**, *34*, D668–D672. [[CrossRef](#)] [[PubMed](#)]
34. Stelzer, G.; Rosen, N.; Plaschkes, I.; Zimmerman, S.; Twik, M.; Fishilevich, S.; Stein, T.I.; Nudel, R.; Lieder, I.; Mazor, Y.; et al. The GeneCards Suite: From Gene Data Mining to Disease Genome Sequence Analyses. *Curr. Protoc. Bioinform.* **2016**, *54*, 1.30.31–31.30.33. [[CrossRef](#)] [[PubMed](#)]
35. Database resources of the National Center for Biotechnology Information. *Nucleic Acids Res.* **2018**, *46*, D8–D13. [[CrossRef](#)]
36. Queralt-Rosinach, N.; Piñero, J.; Bravo, À.; Sanz, F.; Furlong, L.I. DisGeNET-RDF: Harnessing the innovative power of the Semantic Web to explore the genetic basis of diseases. *Bioinformatics* **2016**, *32*, 2236–2238. [[CrossRef](#)]
37. Shannon, P.; Markiel, A.; Ozier, O.; Baliga, N.S.; Wang, J.T.; Ramage, D.; Amin, N.; Schwikowski, B.; Ideker, T. Cytoscape: A software environment for integrated models of biomolecular interaction networks. *Genome Res.* **2003**, *13*, 2498–2504. [[CrossRef](#)]
38. Huang, W.; Sherman, B.T.; Lempicki, R.A. Systematic and integrative analysis of large gene lists using DAVID bioinformatics resources. *Nat. Protoc.* **2009**, *4*, 44–57. [[CrossRef](#)] [[PubMed](#)]
39. Kanehisa, M.; Furumichi, M.; Sato, Y.; Ishiguro-Watanabe, M.; Tanabe, M. KEGG: Integrating viruses and cellular organisms. *Nucleic Acids Res.* **2021**, *49*, D545–D551. [[CrossRef](#)]
40. Szklarczyk, D.; Gable, A.L.; Lyon, D.; Junge, A.; Wyder, S.; Huerta-Cepas, J.; Simonovic, M.; Doncheva, N.T.; Morris, J.H.; Bork, P.; et al. STRING v11: Protein-protein association networks with increased coverage, supporting functional discovery in genome-wide experimental datasets. *Nucleic Acids Res.* **2019**, *47*, D607–D613. [[CrossRef](#)]
41. Burley, S.K.; Bhikadiya, C.; Bi, C.; Bittrich, S.; Chen, L.; Crichlow, G.V.; Christie, C.H.; Dalenberg, K.; Di Costanzo, L.; Duarte, J.M.; et al. RCSB Protein Data Bank: Powerful new tools for exploring 3D structures of biological macromolecules for basic and applied research and education in fundamental biology, biomedicine, biotechnology, bioengineering and energy sciences. *Nucleic Acids Res.* **2020**, *49*, D437–D451. [[CrossRef](#)]
42. Elkins, J.M.; Soundararajan, M.; Vollmar, M.; Krojer, T.; Bountra, C.; Edwards, A.M.; Arrowsmith, C.; Knapp, S. RCSB PDB—6HDR: Human DYRK2 Bound to Curcumin. RCSB PDB, 2019. Available online: <https://www.rcsb.org/structure/6HDR> (accessed on 29 August 2021).
43. Ciccone, L.; Tepshi, L.; Nencetti, S.; Stura, E.A. Transthyretin complexes with curcumin and bromo-estradiol: Evaluation of solubilizing multicomponent mixtures. *New Biotechnol.* **2015**, *32*, 54–64. [[CrossRef](#)] [[PubMed](#)]
44. *The PyMOL Molecular Graphics System*; Schrödinger, LLC: New York, NY, USA.
45. Hanwell, M.D.; Curtis, D.E.; Lonie, D.C.; Vandermeersch, T.; Zurek, E.; Hutchison, G.R. Avogadro: An advanced semantic chemical editor, visualization, and analysis platform. *J. Cheminform.* **2012**, *4*, 17. [[CrossRef](#)] [[PubMed](#)]
46. *BIOVIA Discovery Studio*; Dassault Systèmes: San Diego, CA, USA, 2020.
47. Trott, O.; Olson, A.J. AutoDock Vina: Improving the speed and accuracy of docking with a new scoring function, efficient optimization, and multithreading. *J. Comput. Chem.* **2010**, *31*, 455–461. [[CrossRef](#)]
48. Dallakyan, S.; Olson, A.J. Small-molecule library screening by docking with PyRx. *Methods Mol. Biol.* **2015**, *1263*, 243–250. [[PubMed](#)]
49. Tian, W.; Chen, C.; Lei, X.; Zhao, J.; Liang, J. CASTp 3.0: Computed atlas of surface topography of proteins. *Nucleic Acids Res.* **2018**, *46*, W363–W367. [[CrossRef](#)] [[PubMed](#)]